Tuning of Transmission Responses of an Optical Microring With Negligible Wavelength Shift

Lei Zhao, Simin Li, De Ben, and Shilong Pan, *Senior Member, IEEE*

***Abstract*— The tuning of transmission response of an optical microring resonator (MRR) always associates with significant shift of the resonant wavelength, which leads to serious problems for most of applications. In this letter, we demonstrate that the Mach–Zehnder-interferometer (MZI)-coupled microring resonators with asymmetric directional couplers in the MZIs could still have large magnitude and phase tuning range, while maintaining the resonant wavelength unchanged. An add-drop MZI-coupled microring resonator with asymmetric directional couplers is fabricated on a silicon-on-insulator chip, and the measurement agrees well with the theoretical prediction. Our study would be interesting to photonic integrated circuits, which require tunable MRRs.**

***Index Terms*— Integrated optics, optics resonators, transmission response, tunable.**

I. Introduction

OPTICAL microring resonators (MRRs) are regarded as basic building blocks in integrated photonics for their wide applications in modulators [1], optical filters [2], switches [3], optical delay lines [4], and optical sensors [5]. Coupling coefficients are fundamental parameters of an MRR which determine its finesse, extinction ratio, as well as group delay. One of the effective methods to accurately control the coupling coefficient is to introduce a Mach-Zehnder-interferometer (MZI) coupler into the MRR [6], because the coupling coefficient can be readily adjusted by changing the phase difference between the two arms of the MZI. However, the shift of the resonant wavelength is usually significant during the tuning process [7], [8], which is undesirable to applications requiring a fixed resonant wavelength, such as MRR-based optical delay lines [9], photonic fractional differentiators [10] and optical gyroscopes [11]. For example, the group delay of an MRR-based optical delay line is generally tuned by the coupling coefficients, but the associated resonant wavelength shift will make the actual delay deviated from the targeted value and introduce distortion to the injected signal. To solve this problem, a phase shifter should be inserted into the MRR to compensate the wavelength shift [7], which greatly increases the fabrication difficulty and complicates the operation. The wavelength shift problem can also be overcome by a pull-push tuning method [12], [13], but the difficulty of controlling is also significantly increased and it is only applicable for a critical 50:50 coupler. Reference [8] predicted in theory and demonstrated using numerical simulation that the wavelength shift range of an all-pass MRR is dependent on the configuration of the MRR, indicating a way to solve the wavelength shift problem by designing the architecture of the MRR. However, only an all-pass MRR with notch response is studied, and no experimental investigation is performed.

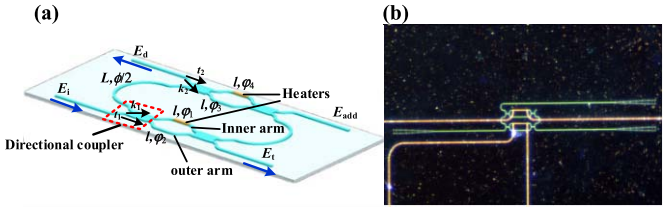

Fig. 1. (a) Schematic diagram of the add-drop MZI-MRR. (b) Photo of the fabricated add-drop MZI-MRR.

In this letter, we theoretically and experimentally study the transmission characteristic of an add-drop MZI-coupled MRR (MZI-MRR) with asymmetric directional couplers in the MZIs, which suggests a simple way to tune the frequency responses of MRRs with negligible wavelength shift. In the theoretical study, the influences of the coupling coefficients of the directional couplers and the phase differences between the two arms in the MZIs are analyzed, which indicate that the resonant wavelength is only sensitive to the phase change in one arm of the MZI if the directional couplers in the MZI have asymmetric splitting ratios. An experiment is carried out. The magnitude and group delay responses of a fabricated silicon-on-insulator MZI-MRR are adjusted with very small shift of the resonant wavelength.

II. Theoretical Analysis

Fig. 1 illustrates the schematic diagram of the add-drop MZI-MRR, of which the two coupling regions are implemented by two MZI couplers, respectively. Each MZI coupler consists of two identical directional couplers and two

Manuscript received August 3, 2017; revised October 22, 2017; accepted November 24, 2017. Date of publication November 29, 2017; date of current version January 8, 2018. This work was supported in part by the National Natural Science Foundation of China under Grant 61604072, Grant 61422108, and Grant 61527820, in part by the China Postdoctoral Science Foundation under Grant 2016M590450, in part by the Shanghai Academy of Spaceflight Technology under Grant SAST2015030, and in part by the Fundamental Research Funds for the Central Universities under Grant NJ20150016, Grant NZ2016105 and Grant NS2016045. *(Corresponding authors: Simin Li; Shilong Pan.)*

The authors are with the Key Laboratory of Radar Imaging and Microwave Photonics, Ministry of Education, Nanjing University of Aeronautics and Astronautics, Nanjing 210016, China (e-mail: lisimin@nuaa.edu.cn; pans@ieee.org).

Color versions of one or more of the figures in this letter are available online at http://ieeexplore.ieee.org.

Digital Object Identifier 10.1109/LPT.2017.2778342

1041-1135 © 2017 IEEE. Personal use is permitted, but republication/redistribution requires IEEE permission.
See http://www.ieee.org/publications_standards/publications/rights/index.html for more information.

$$\left|\frac{E_t}{E_i}\right|^2 = \left|\frac{t_1^2\exp(j\varphi_2) - k_1^2\exp(j\varphi_1) - \gamma\,\exp\left[j\,(\phi+\varphi_1+\varphi_2)\right]\left[t_2^2\exp(j\varphi_3) - k_2^2\exp(j\varphi_4)\right]}{1-\gamma\,\exp(j\phi)\left[t_1^2\exp(j\varphi_1) - k_1^2\exp(j\varphi_2)\right]\left[t_2^2\exp(j\varphi_3) - k_2^2\exp(j\varphi_4)\right]}\right|^2 = \frac{M+\gamma^2 N - 2\gamma\,O}{1+\gamma^2 MN - 2\gamma\,O}, \quad (1)$$

$$\left|\frac{E_d}{E_i}\right|^2 = \left|\frac{\sqrt{\gamma}\,t_1 t_2 k_1 k_2\exp\left(j\frac{\phi}{2}\right)\left[\exp(j\varphi_1)+\exp(j\varphi_2)\right]\left[\exp(j\varphi_3)+\exp(j\varphi_4)\right]}{1-\gamma\,\exp(j\phi)\left[t_1^2\exp(j\varphi_1) - k_1^2\exp(j\varphi_2)\right]\left[t_2^2\exp(j\varphi_3) - k_2^2\exp(j\varphi_4)\right]}\right|^2 = \frac{\gamma\,(1-M)\,(1-N)}{1+\gamma^2 MN - 2\gamma\,O}, \quad (2)$$

waveguides with the same length. For simplicity, the directional couplers are assumed as point devices with zero length and zero insertion loss [14], so the relationship between the self-coupling coefficient t and the cross-coupling coefficient k is $t^2 + k^2 = 1$. The splitting ratio of the directional coupler is described as k^2/t^2. The losses of the arms in the MZIs are also assumed to be zero, and the two MZIs are connected by two bend waveguides with lengths of $L/2$ to form a resonant cavity.

According to a transmission matrix approach to analyze the transmission function of an MZI-MRR [15], we can obtain the magnitude responses of the add-drop MZI-MRR at the through port and the drop port, given by (1) and (2), as shown at the top of this page, where

$$M = t_1^4 + k_1^4 - 2t_1^2 k_1^2\cos(\varphi_1 - \varphi_2), \quad (3)$$

$$N = t_2^4 + k_2^4 - 2t_2^2 k_2^2\cos(\varphi_3 - \varphi_4), \quad (4)$$

$$O = t_1^2 t_2^2\cos(\phi+\varphi_1+\varphi_3) + k_1^2 k_2^2\cos(\phi+\varphi_2+\varphi_4) - t_1^2 k_2^2\cos(\phi+\varphi_1+\varphi_4) - t_2^2 k_1^2\cos(\phi+\varphi_2+\varphi_3), \quad (5)$$

t_1 and t_2 are the self-coupling coefficients of the couplers in the lower and upper MZIs, respectively, $\gamma^{0.5}$ is the transmission factor for each bend waveguide ($\gamma = 1$ means that the waveguide is lossless), φ_1, φ_2, φ_3 and φ_4 are the phase changes of the arms in the two MZIs, $\phi/2 = \pi n_{\text{eff}} L/\lambda$ is the phase change of wavelength λ along the bend waveguide, and n_{eff} is the effective refractive index.

For MZI-MRRs, the tuning of the transmission response is implemented by changing the phase difference between the two arms of the MZI [6], which can be theoretically confirmed by Eqs. (1)-(4). But the adjustment of the phases of the arms in the MZIs also leads to resonant wavelength shift, as can be seen from Eq. (5) which contains a wavelength-dependent term ϕ. In the following part, we will show that if $t_i^2 \gg k_i^2$ or $t_i^2 \ll k_i^2$ ($i = 1$ or 2), the transmission response of the MZI-MRR can be adjusted with a very small shift of the resonant wavelength.

First, we fix the parameters of the upper MZI and investigate the influence of the phases of the arms in the lower MZI on the shift of the resonant wavelength. Eq. (5) can be rewritten as

$$O = t_1^2\left[t_2^2\cos(\phi+\varphi_1+\varphi_3) - k_2^2\cos(\phi+\varphi_1+\varphi_4)\right] - k_1^2\left[t_2^2\cos(\phi+\varphi_2+\varphi_3) - k_2^2\cos(\phi+\varphi_2+\varphi_4)\right]. \quad (6)$$

If $t_1^2 \gg k_1^2$, the second item in Eq. (6) makes a very small influence on the value of O, so tuning the phase of the outer arm φ_2 would not change significantly the resonant wavelength. Similarly, for $t_1^2 \ll k_1^2$, the resonant wavelength is insensitive to φ_1 (the inner arm).

Then, the lower MZI is fixed and the phases of the arms in the upper MZI are changed, so we can rearrange Eq. (5) as

$$O = t_2^2\left[t_1^2\cos(\phi+\varphi_1+\varphi_3) - k_1^2\cos(\phi+\varphi_2+\varphi_3)\right] - k_2^2\left[t_1^2\cos(\phi+\varphi_1+\varphi_4) - k_1^2\cos(\phi+\varphi_2+\varphi_4)\right]. \quad (7)$$

With the similar analysis above, we can obtain that when $t_2^2 \gg k_2^2$, the resonant wavelength is insensitive to φ_4 (the outer arm) and when $t_2^2 \ll k_2^2$, the resonant wavelength is insensitive to φ_3 (the inner arm).

Then, the magnitude tuning range of the MZI-MRR for phase tuning of the resonant-wavelength-insensitive arms is investigated. From Eq. (1), the magnitude response at the through port is determined by M and N, which could be changed from 1 to $(t_1^2 - k_1^2)^2$ and $(t_2^2 - k_2^2)^2$, respectively, if the phase of one arm in each MZI is tuned. Since the directional couplers in the MZIs have asymmetric splitting ratios, the tuning ranges of M and N become smaller as compared with the case that directional couplers with symmetric splitting ratio are used. Fortunately, Eq. (5) can be rewritten as

$$O = t_1^2\sqrt{N}\cos(\phi+\theta_1) - k_1^2\sqrt{N}\cos(\phi+\theta_2) = \sqrt{MN}\cos(\phi+\Phi), \quad (8)$$

where

$$\cos(\theta_1) = \frac{t_2^2\cos(\varphi_1+\varphi_3) - k_2^2\cos(\varphi_1+\varphi_4)}{\sqrt{N}}, \quad (9)$$

$$\sin(\theta_1) = \frac{t_2^2\sin(\varphi_1+\varphi_3) - k_2^2\sin(\varphi_1+\varphi_4)}{\sqrt{N}}, \quad (10)$$

$$\cos(\theta_2) = \frac{t_2^2\cos(\varphi_2+\varphi_3) - k_2^2\cos(\varphi_2+\varphi_4)}{\sqrt{N}}, \quad (11)$$

$$\sin(\theta_2) = \frac{t_2^2\sin(\varphi_2+\varphi_3) - k_2^2\sin(\varphi_2+\varphi_4)}{\sqrt{N}}, \quad (12)$$

$$\cos(\Phi) = \frac{t_1^2\cos(\theta_1) - k_1^2\cos(\theta_2)}{\sqrt{M}}, \quad (13)$$

$$\sin(\Phi) = \frac{t_1^2\sin(\theta_1) - k_1^2\sin(\theta_2)}{\sqrt{M}}, \quad (14)$$

so Eq. (1) can be converted to

$$\left|\frac{E_t}{E_i}\right|^2 = \frac{M+\gamma^2 N - 2\gamma\sqrt{MN}\cos(\phi+\Phi)}{1+\gamma^2 MN - 2\gamma\sqrt{MN}\cos(\phi+\Phi)}, \quad (15)$$

From Eq. (15), the resonant wavelength appears at $\cos(\phi+\Phi) = 1$, and a critical coupling state of $\sqrt{M} = \gamma\sqrt{N}$ is existed, which can result in the deepest notch response at

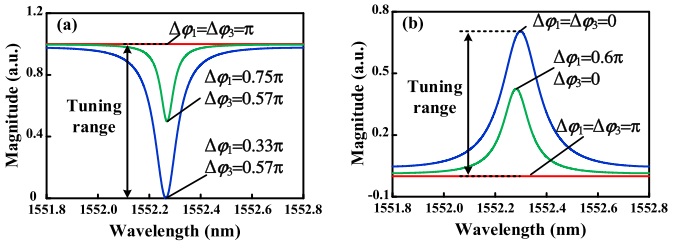

Fig. 2. The magnitude responses of the MZI-MRR for different φ_1 and φ_3 at (a) the through port and (b) the drop port, with $t_1^2 = t_2^2 = 0.1$.

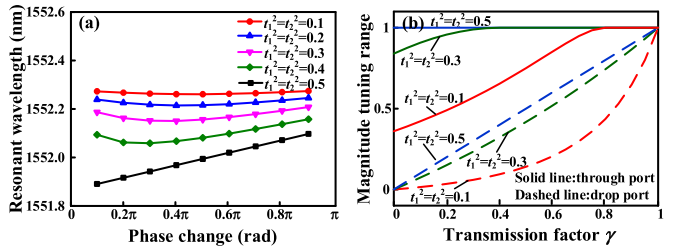

Fig. 3. (a) The resonant wavelength as a function of the phase of the inner arm φ_1, and (b) the magnitude tuning range as a function of the waveguide loss for MRRs with different t_1^2 and t_2^2.

the through port. Take $t_1^2 = t_2^2 = 0.1$ as an example. The amplitude transmission factor is set as $\gamma = 0.92$, φ_2 and φ_4 are fixed at arbitrary value (i.e. uncontrolled) while φ_1 and φ_3 are tuned. The simulation result is shown in Fig. 2(a), which illustrates that the magnitude of the response can be tuning from 1 to 0 with very slight resonant wavelength shift.

For the magnitude response at the drop port, from Eq. (2), the maximum of the magnitude appears at $M = (t_1^2 - k_1^2)^2$ and $N = (t_2^2 - k_2^2)^2$ which cannot be 0 because of the asymmetric splitting ratios, so the tuning range would be smaller than that of a MZI-MRR with symmetric directional couplers (i.e. $t_1^2 = t_2^2 = 0.5$, denoted as normal MZI-MRR hereafter). With the same parameters in Fig. 2(a), the tuning range of the magnitude is calculated to be from 0 to 0.7052, as shown in Fig. 2(b), indicating that the compression of the tuning range of the magnitude response at the drop port is tolerable.

Fig. 3(a) shows the resonant wavelength as a function of the phase of the inner arm φ_1 for directional couplers with different splitting ratios. In the simulation, all the parameters of the MZI-MRR expect for φ_1, t_1 and t_2 maintain unchanged. As can be seen, the resonant wavelength shift range decreases with the decreasing of the splitting ratios of the directional couplers. For an MZI-MRR with critical 50:50 couplers (i.e. $t_1^2 = t_2^2 = 0.5$), the resonant wavelength shift range reaches 0.21 nm, as compared with the wavelength shift of only ~0.01nm for $t_1^2 = t_2^2 = 0.1$.

The influences of the splitting ratio of the directional couplers and the waveguide loss on the magnitude tuning range are also studied, as illustrated in Fig. 3(b). Generally, the magnitude tuning range becomes small with the decreasing of the splitting ratio. However, by reducing the waveguide loss, the magnitude tuning range can be dramatically improved. Take $t_1^2 = t_2^2 = 0.1$ as an example. At the through port, the magnitude response has the same tuning range as a normal

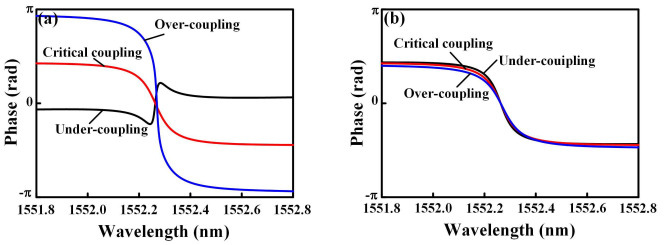

Fig. 4. The phase responses of the MZI-MRR by tuning φ_1 and φ_3 at (a) the through port and (b) the drop port, with $t_1^2 = t_2^2 = 0.1$.

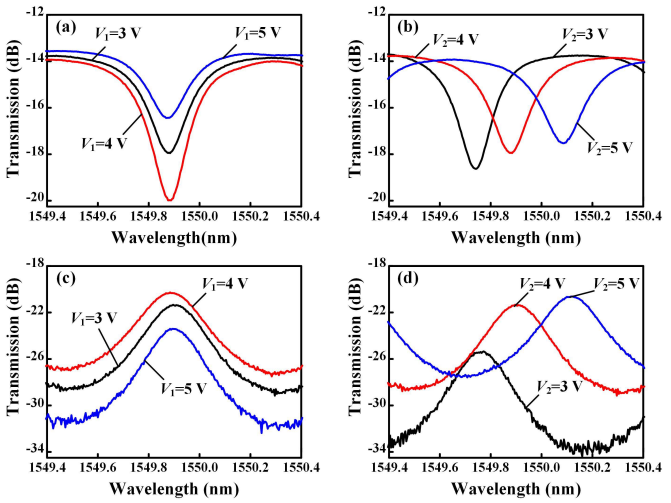

Fig. 5. The measured transmission responses of the add-drop MZI-MRR. In (a) and (c) $V_2 = 4$ V and V_1 changes from 3 to 5 V, in (b) and (d) $V_1 = 3$ V and V_2 changes from 3 to 5 V.

MZI-MRR when $\gamma > 0.8$; and at the drop port, when $\gamma > 0.95$, the magnitude tuning range is about 0.8, which is close to that of a normal MZI-MRR.

The phase responses are also numerically analyzed with cases of $M^{0.5} > \gamma N^{0.5}$, $M^{0.5} = \gamma N^{0.5}$ and $M^{0.5} < \gamma N^{0.5}$, which are defined as under-, critical and over-coupling state, respectively. Fig. 4 shows the simulation results. The phase response at the through port is similar to that of a normal MZI-MRR, which is monotonically decreasing for the over-coupling state and increasing in the center for the under-coupling state. The phase response at the drop port is monotonically decreasing, which is also in accordance with a normal MZI-MRR.

III. Experimental Results

To verify the analysis, an add-drop MZI-MRR with asymmetric directional couplers is fabricated on a silicon-on-insulator chip which is shown in Fig. 1(b). The ring cavity is 651 μm long, corresponding to a free spectral range of 0.9 nm. The coupling coefficient is $t^2 \approx 0.12$. The phase change is tuned by adjusting the voltages (V_1 and V_2) to Ti/Au thermal heaters on the inner arm of the lower MZI and the outer arm of the upper MZI. Fig. 5 shows the measured transmission responses. To obtain Fig. 5(a) and (c), V_2 is fixed at 4 V while V_1 is changed from 3 to 5 V. As can be seen, there are no obvious wavelength shifts for both through and drop ports, where the wavelength shifts 0.007nm.

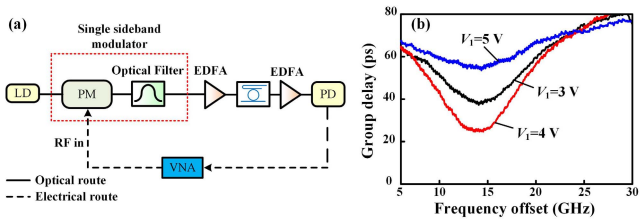

Fig. 6. (a) Schematic diagram of the ultrahigh-resolution optical vector analyzer (OVA) based on optical single-sideband modulation. (b) Group delay as a function of the frequency offset to 1549.77 nm at the through port of the add-drop MZI-MRR for different V_1.

The notch depth of the transmission response obtained at through port increases first and then declines with the increase of V_1 because the tuning arm in the MZI could produce a phase shift of more than π. Then, we fix V_1 at 3 V, and tune V_2 from 3 to 5 V. As can be seen in Fig. 5(b) and (d) which illustrate the frequency responses at the through and drop ports, respectively, there are significant red shifts. The measured results are in good agreement with the simulation.

The group delay response at the through port of the MZI-MRR is measured using an ultrahigh-resolution optical vector analyzer (OVA) based on optical single-sideband (OSSB) modulation [16], as shown in Fig. 6(a). The key component is an OSSB modulator comprising of a phase modulator and an optical bandpass filter, which generates a wavelength-fixed optical carrier and a sideband. When this signal goes through the MZI-MRR, the amplitude and phase of the sideband change according to the frequency response of the MZI-MRR. Then, the optical signal is converted into an electrical signal at a photodetector (PD), where the amplitude and phase information is extracted by a microwave phase-magnitude detector in the VNA. By sweeping the frequency of the RF source, the phase and amplitude responses of the MZI-MRR can be obtained in the electrical domain. The measured wavelength range is 30 GHz, which is limited by the bandwidth of the PD. Fig. 6(b) shows the measured group delay responses. Here, the group delay τ_g is defined as $\tau_g = -\mathrm{d}\varphi/\mathrm{d}\omega$, where φ is the phase and ω is the angular frequency. By increasing V_1 on the inner arm of the lower MZI while maintaining a fixed V_2, the group delay at the through port changes with a very small shift of the center wavelength. It should be noted that the three measured group delay curves are all corresponding to the under-coupling phase responses in Fig. 4(a). The possible reason is that the waveguide loss is large, i.e., the transmission factor γ is small, subject to our relatively low fabrication accuracy, which keeps the MZI-MRR in the state of $M^{0.5} > \gamma N^{0.5}$.

IV. Conclusions

In summary, we demonstrated a method to overcome the wavelength shift problem of MZI-MRRs caused by tuning of the magnitude and phase responses by applying directional couplers with asymmetric splitting ratios in the MZIs. Theoretical and experimental results show that the magnitude and the phase responses of the MZI-MRR can be controlled by the phase of each arm in the MZIs, while the resonant wavelength is only sensitive to the phase of one arm. As a result, the properties of the MZI-MRR can be adjusted while maintaining the resonant wavelength unchanged by tuning the phases of the insensitive arms. The proposed approach would be interesting to the applications of the tunable MRRs which requires a stable resonant wavelength.

References

[1] L. Chen, Q. Xu, M. G. Wood, and R. M. Reano, "Hybrid silicon and lithium niobate electro-optical ring modulator," *Optica*, vol. 1, no. 2, pp. 112–118, Aug. 2014.
[2] N. Eid, R. Boeck, H. Jayatilleka, L. Chrostowski, W. Shi, and N. A. F. Jaeger, "FSR-free silicon-on-insulator microring resonator based filter with bent contra-directional couplers," *Opt. Exp.*, vol. 24, no. 25, pp. 29009–29021, Dec. 2016.
[3] Y. Vlasov, W. M. J. Green, and F. Xia, "High-throughput silicon nanophotonic wavelength-insensitive switch for on-chip optical networks," *Nature Photon.*, vol. 2, no. 4, pp. 242–246, 2008.
[4] M. Burla *et al.*, "On-chip CMOS compatible reconfigurable optical delay line with separate carrier tuning for microwave photonic signal processing," *Opt. Exp.*, vol. 19, no. 22, pp. 21475–21484, Oct. 2011.
[5] J. Wang and D. Dai, "Highly sensitive Si nanowire-based optical sensor using a Mach–Zehnder interferometer coupled microring," *Opt. Lett.*, vol. 35, no. 24, pp. 4231–4299, Dec. 2010.
[6] D. Dai and S. He, "Highly sensitive sensor based on an ultra-high-Q Mach–Zehnder interferometer-coupled microring," *J. Opt. Soc. Amer. B, Opt. Phys.*, vol. 26, no. 3, pp. 511–516, Mar. 2009.
[7] H. Takahashi, R. Inohara, K. Nishimura, and M. Usami, "Expansion of bandwidth of tunable dispersion compensator based on ring resonators utilizing negative group delay," *J. Lightw. Technol.*, vol. 24, no. 6, pp. 2276–2286, Jun. 2002.
[8] X.-Y. Zhang, T. Zhang, X.-J. Xue, Y.-P. Cui, and P.-Q. Wu, "Resonant frequency shift characteristic of integrated optical ring resonators with tunable couplers," *J. Opt. A, Pure Appl. Opt.*, vol. 11, no. 8, p. 085411, Aug. 2009.
[9] H. Takahashi, P. Carlsson, K. Nishimura, and M. Usami, "Analysis of negative group delay response of all-pass ring resonator with Mach–Zehnder interferometer," *IEEE Photon. Technol. Lett.*, vol. 16, no. 9, pp. 2063–2065, Sep. 2004.
[10] B. Jin *et al.*, "A comprehensive theoretical model for on-chip microring-based photonic fractional differentiators," *Sci. Rep.*, vol. 5, Sep. 2015, Art. no. 14216.
[11] K. Suzuki, K. Takiguchi, and K. Hotate, "Monolithically integrated resonator microoptic gyro on silica planar lightwave circuit," *J. Lightw. Technol.*, vol. 8, no. 1, pp. 66–72, Jan. 2000.
[12] M. Abouzahra and L. Lewin, "Theory and application of coupling between curved transmission lines," *IEEE Trans. Microw. Theory Techn.*, vol. MTT-30, no. 11, pp. 1988–1995, Nov. 1982.
[13] A. Yariv, "Critical coupling and its control in optical waveguide-ring resonator systems," *IEEE Photon. Technol. Lett.*, vol. 14, no. 4, pp. 483–485, Apr. 2002.
[14] W. D. Sacher and J. K. S. Poon, "Characteristics of microring resonators with waveguide-resonator coupling modulation," *J. Lightw. Technol.*, vol. 27, no. 17, pp. 3800–3811, Sep. 1, 2009.
[15] L. Zhou and A. W. Poon, "Electrically reconfigurable silicon microring resonator-based filter with waveguide-coupled feedback," *Opt. Exp.*, vol. 15, no. 15, pp. 9194–9204, Jul. 2007.
[16] S. Pan and M. Xue, "Ultrahigh-resolution optical vector analysis based on optical single-sideband modulation," *J. Lightw. Technol.*, vol. 35, no. 4, pp. 836–845, Feb. 15, 2017.